Electronic Supplementary Material (ESI) for Journal of Materials Chemistry B.

Supporting Information

Structural Engineering of Mitochondria-Targeted Au-Ag_2S Photosensitizers for Enhanced Photodynamic and Photothermal Therapy

Ruofei Ma, Qi Zhang, Yue Wang and Zhangrun Xu**

Department of Chemistry, College of Sciences, Northeastern University, Shenyang, Liaoning, 110819, China

*E-mail: yuewang@mail.neu.edu.cn and xuzr@mail.neu.edu.cn

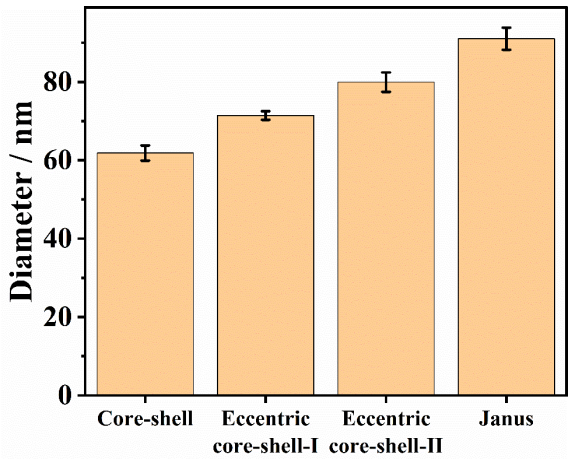

Figure S1. The long-axis diameters of AICM NPs with core-shell, eccentric core-shell-I, eccentric core-shell-II, and Janus morphologies.

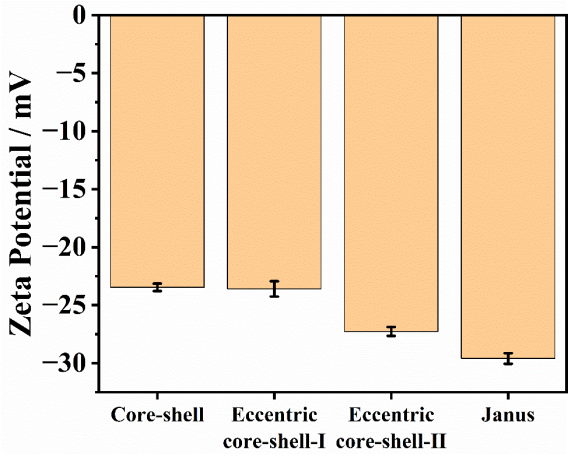

Figure S2. The zeta potentials of AICM NPs with core-shell, eccentric core-shell-I, eccentric core-shell-II, and Janus morphologies.

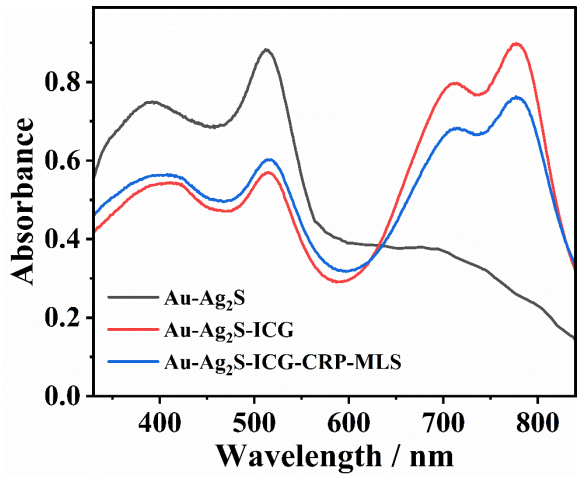

Figure S3. UV-vis absorption spectra of Au-Ag_2S, Au-Ag_2S-ICG, and Au-Ag_2S-ICG-CRP-MLS.

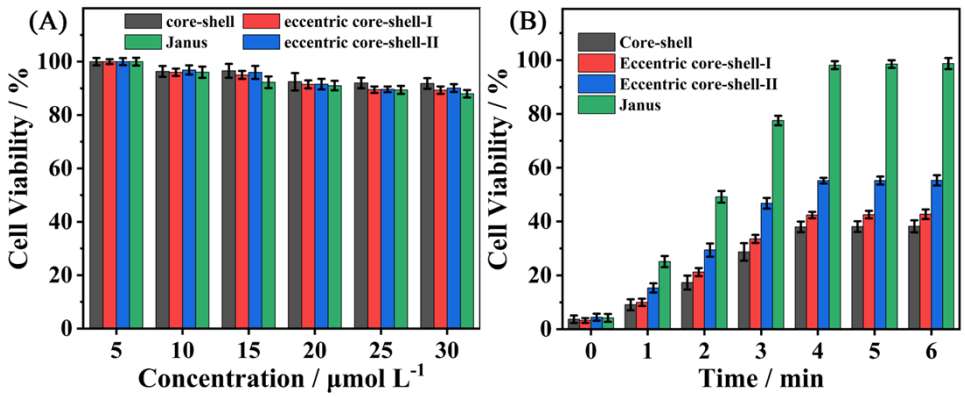

Figure S4. (A) Effect of different concentrations of AICM NPs with different morphologies on viabilities of LoVo cells after incubation for 24 h. The error bars indicate the standard deviations of three parallel experiments. (B) The apoptosis rate PDT and PTT 0-6 min by AICM NPs with different morphologies at different times. The error bars indicate the standard deviations of three parallel experiments.

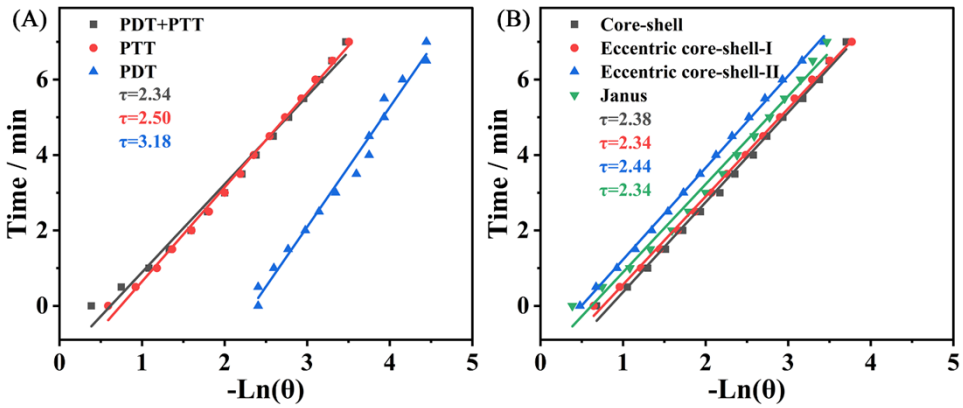

Figure S5. (A) The corresponding fitting curves of PDT, PTT and PDT + PTT group are based on Roper's method for photothermal conversion time constants calculation. (B) The corresponding fitting curves of AICM NPs with different morphologies are based on Roper's method for photothermal conversion time constants calculation.

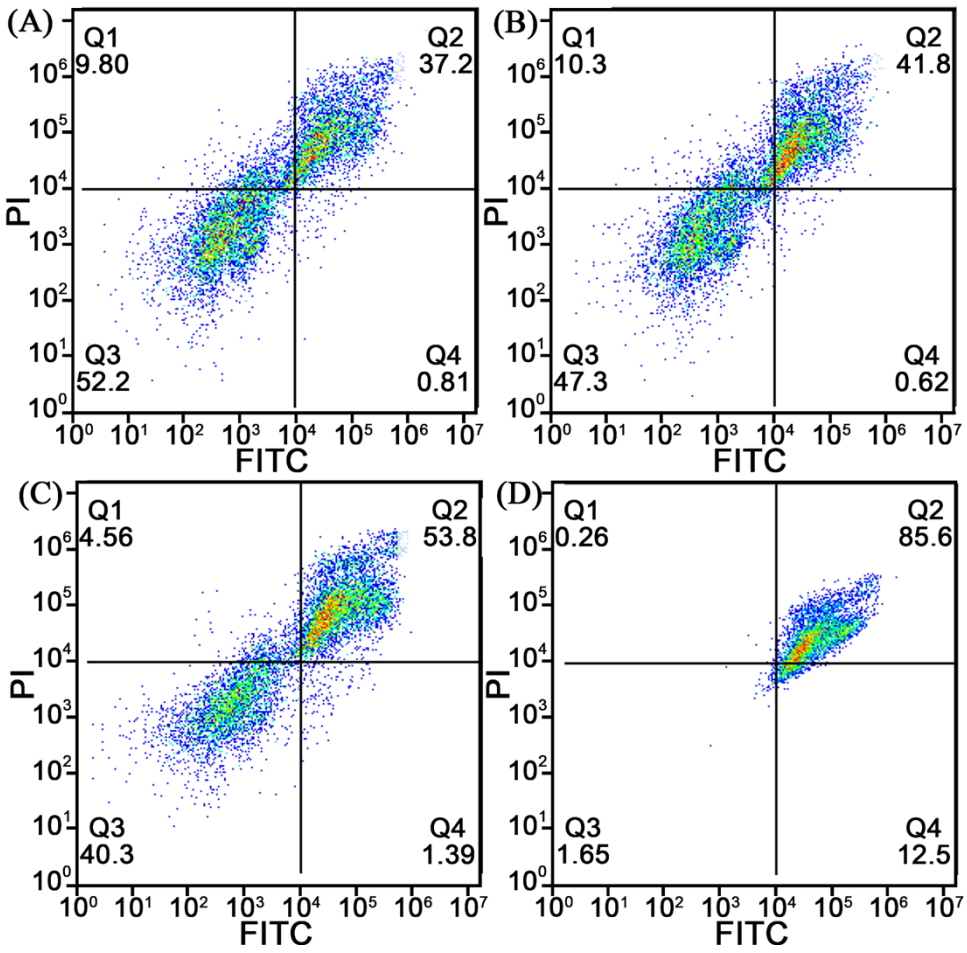

Figure S6. The flow cytometry patterns of LoVo cells treated by AICM NPs with (A) core-shell, (B) eccentric core-shell-I, (C) eccentric core-shell-II and (D) Janus morphologies.

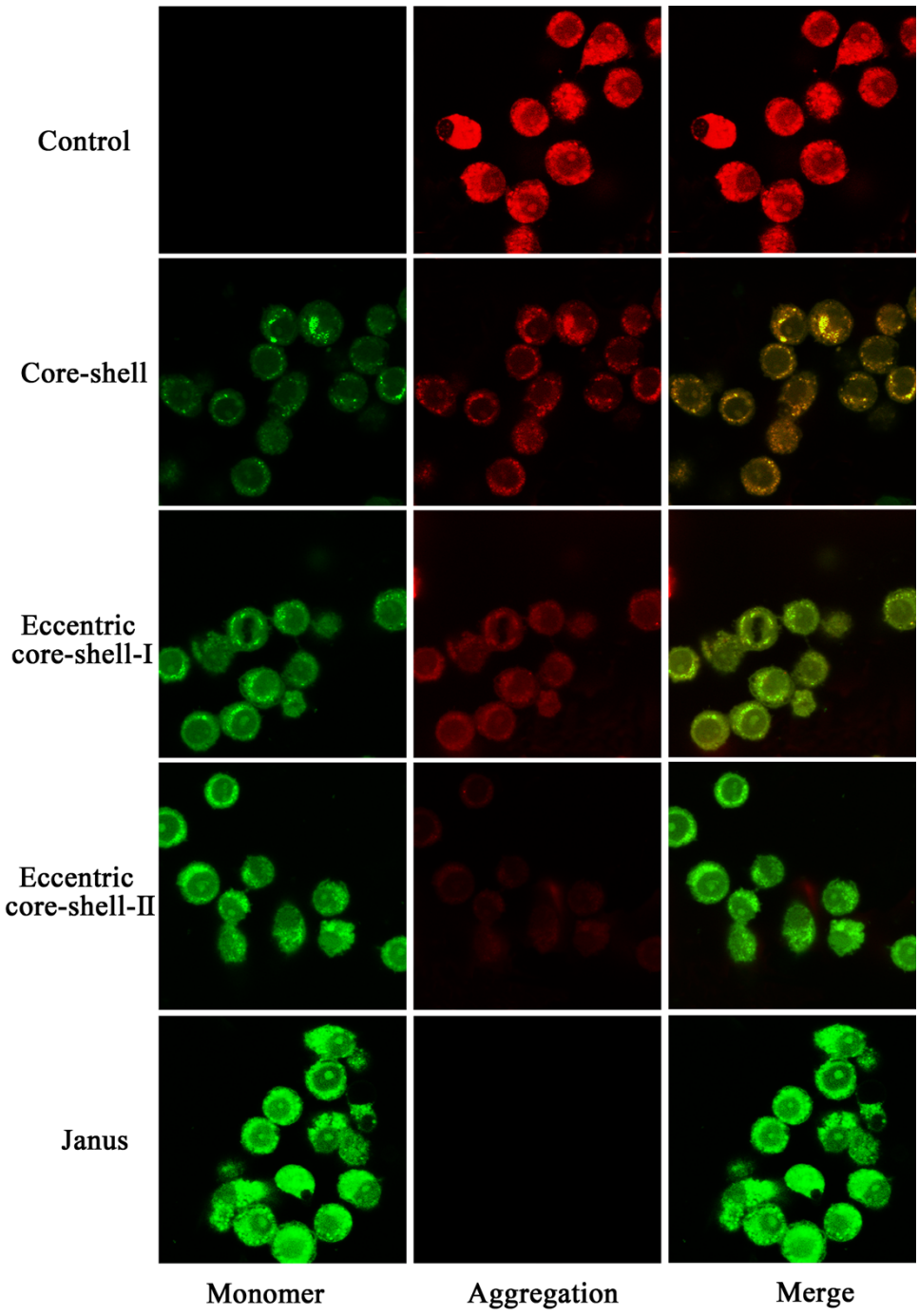

Figure S7. Fluorescence images of JC-1 stained LoVo cells with Core-shell, Eccentric core-shell-I, Eccentric core-shell-II, and Janus groups.

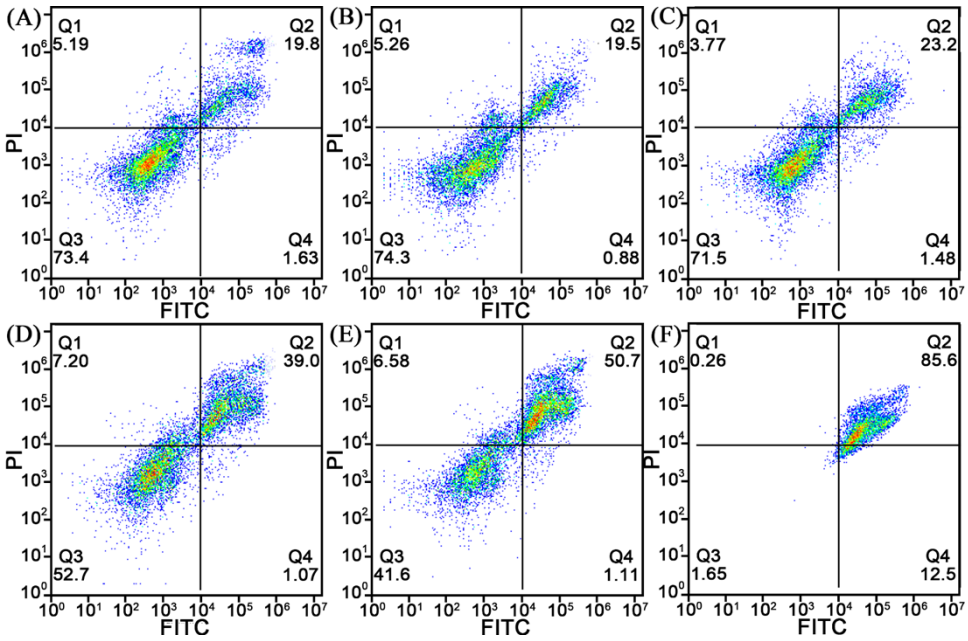

Figure S8. The flow cytometry patterns of LoVo cells treated by (A) Control, (B) AICM NPs, (C) Laser, (D) PDT, (E) PTT, and (F) PDT + PTT group.

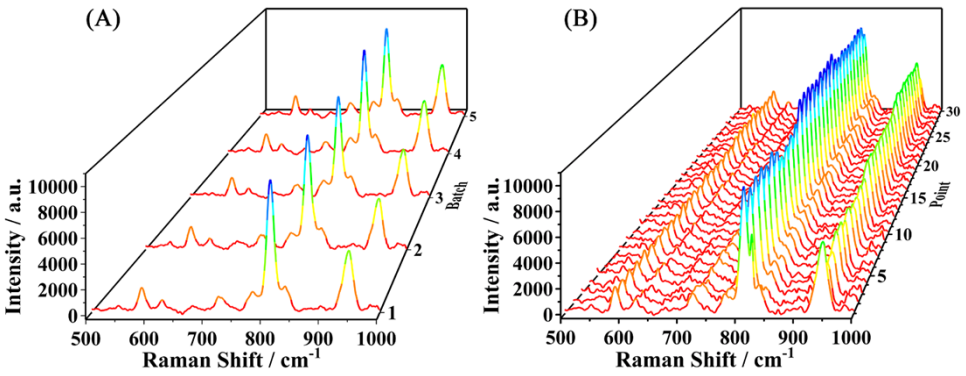

Figure S9. (A) SERS spectra of AICM NPs measured from 5 different batch substrates. (B) SERS spectra of AICM NPs measured from 30 different points.

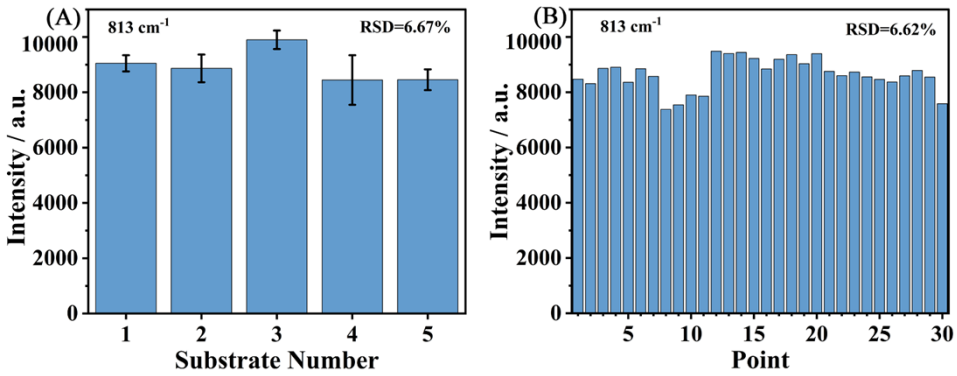

Figure S10. (A) Histogram of SERS intensity at 813 cm^{-1} measured from 5 different batch substrates. (B) Histogram of SERS intensity at 813 cm^{-1} measured from 30 different points.

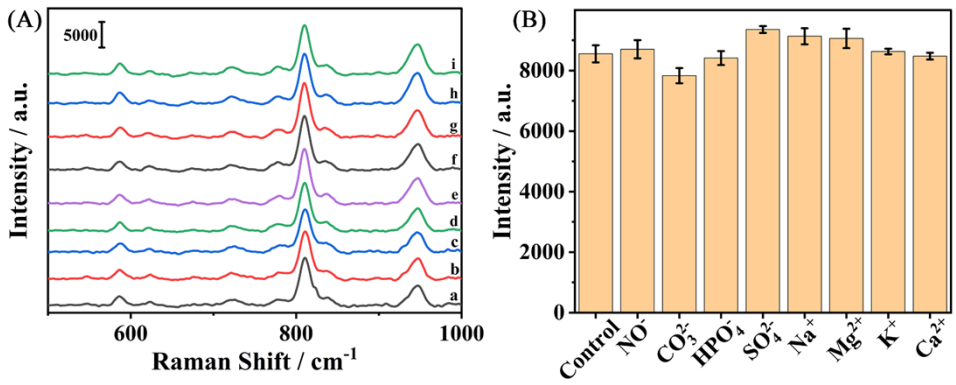

Figure S11. (A) SERS spectra of AICM NPs with Janus morphology with caspase-3 and different ionic groups (a: Control group; b: NO^-; c: CO_3^{2-}; d: HPO_4^-; e: SO_4^{2-}; f: Na^+; g: Mg^{2+}; h: Ka^+; i: Ca^{2+}; n=10). (B) Histogram of SERS intensity at 813 cm^{-1} for the AICM NPs with Janus morphology treated with caspase-3 and different anions (n=10).

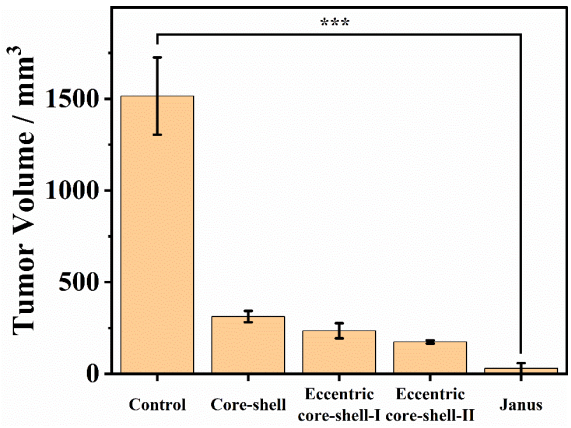

Figure S12. The tumor sizes after treatment by AICM NPs with different morphologies. *** $p < 0.001$.

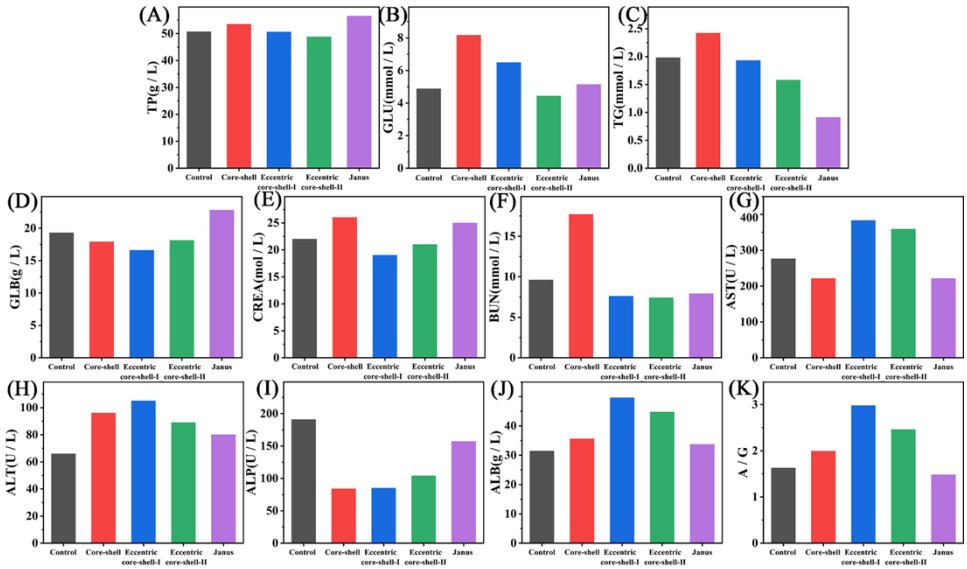

Figure S13. Blood biochemical analysis for mice in Control, Core-shell, Eccentric core-shell-I, Eccentric core-shell-II, and Janus groups 10 days post therapy: (A) total protein (TP), (B) blood glucose (GLU), (C) triglyceride (TG), (D) globulin (GLB), (E) creatinine (CREA), (F) urea nitrogen (BUN), (G) aspartate aminotransferase (AST), (H) alanine aminotransferase (ALT), (I) alkaline phosphatase (ALP), (J) albumin (ALB) and (K) albumin and globulin ratio (A/G).

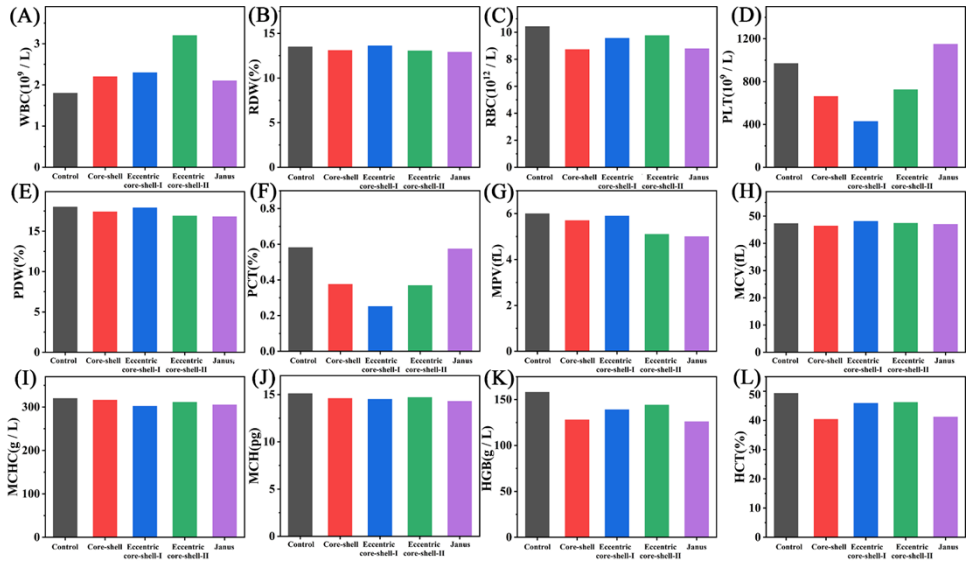

Figure S14. Hematological analysis for mice in Control, Core-shell, Eccentric core-shell-I, Eccentric core-shell-II, and Janus groups 10 days post therapy: (A) white blood cell (WBC), (B) red blood cell volume distribution width (RDW), (C) red blood cell (RBC), (D) platelet (PLT), (E) hemoglobin (HGB), (F) plateletcrit (PCT), (G) mean platelet volume (MPV), (H) mean corpuscular volume (MCV), (I) mean corpuscular hemoglobin concentration (MCHC), (J) mean corpuscular hemoglobin (MCH), (K) platelet distribution width (PDW) and (L) hematocrit (HCT).

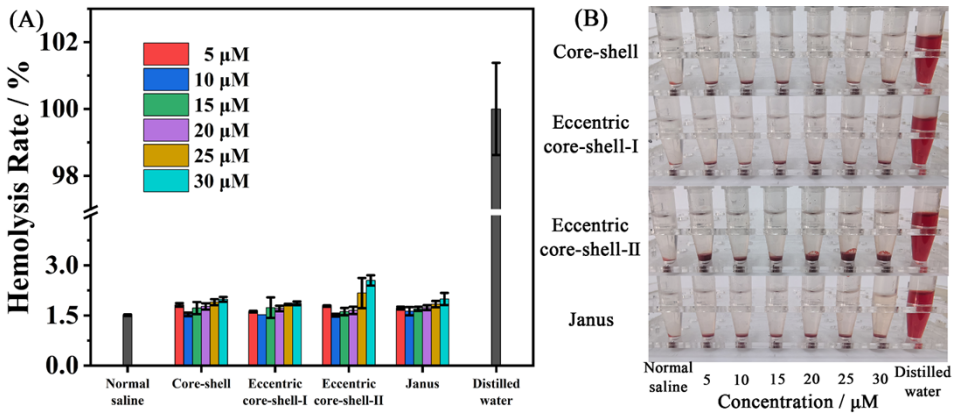

Figure S15. (A) The percentage of hemolysis rates of AICM NPs with different morphologies. (B) Hemocompatibility results of AICM NPs with different morphologies.

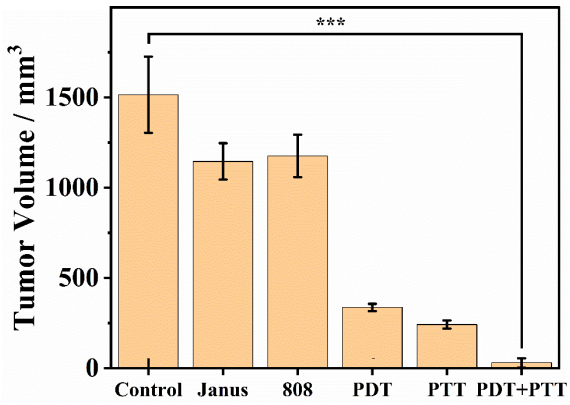

Figure S16. The tumor sizes after various treatments. *** $p < 0.001$.

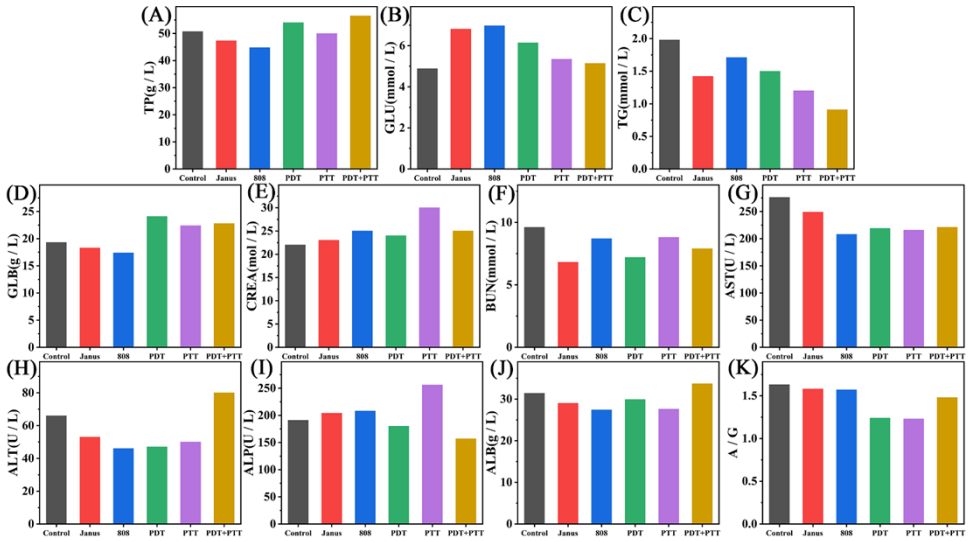

Figure S17. Blood biochemical analysis for mice in Control, AICM NPs, Laser, PDT, PTT and PDT + PTT groups 10 days post therapy: (A) TP, (B) GLU, (C) TG, (D) GLB, (E) CREA, (F) BUN, (G) AST, (H) ALT, (I) ALP, (J) ALB and (K) A/G.

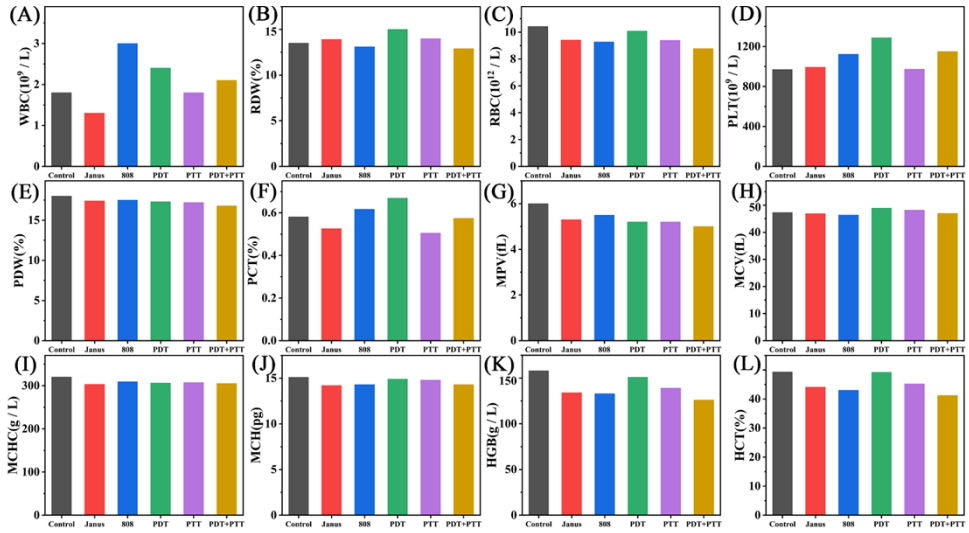

Figure S18. Hematological analysis for mice in Control, AICM NPs, Laser, PDT, PTT and PDT + PTT groups 10 days post therapy: (A) WBC, (B) RDW, (C) RBC, (D) PLT, (E) HGB, (F) PCT, (G) MPV, (H) MCV, (I) MCHC, (J) MCH, (K) PDW and (L) HCT.

Table S1. Comparison of therapy performances

PS	Therapy	Time of in vitro treatment (days)	Apoptosis rate of in vivo treatment	Ref.
MLP@DHA&Ce_6	PDT+CDT	20	77.1%	[1]
Rh-BI	PDT+PTT	21	30%	[2]
2TPEVDPP NPs	PDT+PTT	18	67.96%	[3]
UCNPs-YS@ZnPc@TPZ	PDT+ICD	19	75%	[4]
AICM NPs	PDT+PTT	10	98.1%	This work

References

1 G. Liu, M. Liu, X. Li, X. Ye, K. Cao, Y. Liu and Y. Yu, *ACS Appl. Mater. Interfaces*, 2023, **15**, 47955-47968.

2 M. Zhang, S. Wang, Y. Bai, D. Wang, Y. Fu, Z. Su, G. Zhang, M. Meng, F. Yu, B. Wang, H. Jin and W. Zhao, *Adv. Healthc. Mater.*, 2023.

3 L. Feng, C. Li, L. Liu, Z. Wang, Z. Chen, J. Yu, W. Ji, G. Jiang, P. Zhang, J. Wang and B. Z. Tang, *ACS Nano*, 2022, **16**, 4162-4174.

4 C. Wu, M. Cui, L. Cai, C. Chen, X. Zhu, Y. Wu, J. Liu, H. Wang and Y. Zhang, *ACS Appl. Mater. Interfaces*, 2022, **14**, 13094-13106.